

MPI-PhT/94-33

LMU-09/94

June 1994

Search for new physics in e^-e^- scattering¹

F. Cuyppers^a, K. Kołodziej^{b,2,3} and R. Rückl^{a,b,2}

^a*Max-Planck-Institut für Physik, Werner-Heisenberg-Institut,
Föhringer Ring 6, D-80805 München, FRG*

^b*Sektion Physik der Universität München,
Theresienstr. 37, D-80333 München, FRG*

Abstract

Considering the physics potential of an e^-e^- collider in the TeV energy range, we indicate a few interesting examples for exotic processes and discuss the standard model backgrounds. Focussing on pair production of weak gauge bosons, we report some illustrative predictions.

¹Talk presented by K. Kołodziej at the Zeuthen Workshop on Elementary Particle Theory, ‘*Physics at LEP200 and Beyond*’, Teupitz, Germany, 10–15 April, 1994

² Work supported by the German Federal Ministry for Research and Technology under contract No. 05 6MU 93P

³ On leave from the Institute of Physics, University of Silesia, ul. Uniwersytecka 4, PL-40007 Katowice, Poland

1 Introduction

The prospects of experimentation at an e^+e^- linear collider facility are exciting, not the least because of the possibility to collide in addition to e^+ and e^- beams also e^- with e^- , e^- with γ , and γ with γ beams. Whereas much theoretical work has already been dedicated to e^+e^- , $e\gamma$ and $\gamma\gamma$ physics [1], the e^-e^- option has not yet been studied comprehensively. One reason for this is the symmetry constraint in the standard model which to lowest order allow only for Møller scattering. However, it is just this fact which makes e^-e^- scattering very advantageous for new physics searches.

In this talk we indicate interesting nonstandard scenarios which could be tested in e^-e^- collisions. We also discuss the main standard model backgrounds, except for the rather harmless Møller scattering and Bremsstrahlung processes. Moreover, we concentrate on the weak boson pair production processes $e^-e^- \rightarrow W^-W^- \nu_e \nu_e$, $W^-Z^0 e^- \nu_e$ and $Z^0Z^0 e^-e^-$ for which we are able to report new results [2, 3].

2 New physics reactions

A major virtue of e^-e^- scattering as compared to the other reactions to be achieved at a linear collider, is its particular sensitivity to lepton-number violating processes. For example, the existence of heavy Majorana neutrinos which mix with the known neutrino species would increase the W^-W^- pair production rate by inducing the reaction $e^-e^- \rightarrow W^-W^-$ [4, 5]. In particular, this process is expected to occur in the framework of left-right symmetric models, whose lagrangians naturally incorporate right-handed neutrinos and Majorana mass terms, and in which the light mass eigenstate W^- is a mixing of W_L^- and W_R^- . The production of a heavy mass eigenstate W'^- is also an interesting possibility at higher energies [4, 6]. Another example emerges in grand-unified models which contain dileptons among the heavy gauge bosons. These states give rise to electron-number violating transitions of the kind $e^-e^- \rightarrow \mu^-\mu^-$ [7]. The latter process can also be mediated in left-right symmetric models by doubly charged Higgs boson exchange and higher order contributions from box diagrams involving Majorana neutrinos and the charged gauge bosons $W_{L,R}^-$ [8]. Furthermore, in supersymmetric models, lepton-number violating processes can take place via the exchange of sneutrinos leading to chargino pair production in $e^-e^- \rightarrow \tilde{\chi}^-\tilde{\chi}^-$ [9].

However, also lepton-number conserving processes can give insight into new physics. For instance, the reaction $e^-e^- \rightarrow e^-W^-\nu_e$ allows for tests of possible anomalous boson couplings which are complementary to those in e^+e^- , $e\gamma$ and $\gamma\gamma$ collisions [10]. In addition, selectron pair production in $e^-e^- \rightarrow \tilde{e}^-\tilde{e}^-$ proceeding by the exchange of neutralinos, would provide a background-free supersymmetric signal and a measurement of the neutralino mass [9, 11]. Similarly, stronger constraints than in e^+e^- can be obtained for an additional Z' boson [12]. In the following we will discuss some of the above reactions in more detail.

2.1 $e^-e^- \rightarrow W^-W^-$

Heavy Majorana neutrinos are naturally incorporated in the framework of left-right symmetric gauge models [4, 6] or $SO(10)$ GUTs [5]. The production of W^- pairs is then mediated by t -channel exchange of Majorana neutrinos and s -channel exchange of a doubly charged Higgs boson Δ^{--} , as depicted in Fig. 1. The latter mainly affects the high energy behaviour of the cross sections due to interference with the neutrino exchange amplitudes. The physical neutrino mass eigenstates are mixtures of the known light neutrino flavours and the new heavy states. Contributions from the exchange of light neutrino eigenstates are suppressed by minute mixing angles of light and heavy neutrinos (and/or of W_L^- and W_R^- in the case of $e_L^-e_R^-$). These mixing angles are strongly constrained by the nonobservation of neutrinoless double β -decay [5].

Restricting oneself to the ‘low’ energy region, $2m_W \ll \sqrt{s} \ll m_{\nu_M}$, one can neglect the charged Higgs contribution. Neglecting also W_L^- and W_R^- mixing, the cross section for unpolarized electrons and heavy neutrino exchange is estimated to be [5]

$$\sigma^N = \frac{G_F^2 s}{16\pi M_{\text{red}}^2} |\eta_N|^2. \quad (1)$$

Here, $M_{\text{red}}^{-1} = \sum_i M_i^{-1}$ denotes the inverse of the reduced mass of heavy neutrinos which are assumed to have masses in the 1 TeV range, and η_N is a dimensionless neutrino mixing parameter. For $|\eta_N| \leq (2-40) \cdot 10^{-4}$, the maximal mixing compatible with low energy data [5], one obtains the following order of magnitude estimates:

$$\sigma^N \leq \begin{cases} 0.01 - 4 \text{ fb} & \text{at } \sqrt{s} = 0.5 \text{ TeV} \\ 0.16 - 64 \text{ fb} & \text{at } \sqrt{s} = 1 \text{ TeV}. \end{cases} \quad (2)$$

2.2 $e^-e^- \rightarrow \tilde{e}^-\tilde{e}^-$ or $\tilde{\chi}^-\tilde{\chi}^-$

In the supersymmetric extension of the standard model selectrons and charginos are produced in pairs, as depicted in Fig. 2.

Selectron pair production proceeds via the t - and u -channel exchange of neutralinos. Note that this reaction also violates fermion-number conservation, which comes as no surprise since the neutralinos are Majorana fermions. The cross section for $e^-e^- \rightarrow \tilde{e}^-\tilde{e}^-$ depends very crucially on the properties of the exchanged neutralinos [13], *i.e.* their masses and mixing. In the minimal model, the masses $m_{\tilde{\chi}_i^0}$ of the four neutralino states ($i = 1, 2, 3, 4$) and their couplings $g_{iL,R}$ to electron-selectron pairs of left (L) and right (R) chiralities are complicated functions of supersymmetry parameters [14].

Chargino pair production proceeds via the t - and u -channel exchange of a sneutrino. Since charginos only couple to left-handed leptons, only the LL component of a given e^-e^- initial state contributes. Again, the masses $m_{\tilde{\chi}_i^\pm}$ of the charginos and their couplings

to selectrons g_i are determined by the supersymmetric parameters relevant also in the neutralino sector.

In Fig. 3, taken from Ref. [9], we show the energy dependence of the selectron and chargino production cross sections for varying selectron and sneutrino masses. For the ratio of the Higgs vacuum expectation values we assume $v_2/v_1 = \tan \beta = 10$, for the Higgs/higgsino mass parameter $\mu = -300$ GeV and for the mass parameter of the $SU(2)_L$ gaugino sector $M_2 = 300$ GeV. The corresponding mass parameter M_1 of the $U(1)_Y$ gaugino sector is related to M_2 by evolving both from a common value $M_1 = M_2$ at the grand unification scale, to the relevant low energy scale with the help of renormalization group equations.

3 Standard model processes

As already mentioned in the Introduction, in the framework of the standard model, the majority of events in e^-e^- collisions arise from Møller scattering accompanied by Bremsstrahlung:

$$e^-e^- \rightarrow e^-e^-(\gamma). \quad (3)$$

This background can be efficiently suppressed by imposing acollinearity and/or acoplanarity cuts.

Next most important is the production and decay of single gauge bosons in the reactions

$$e^-e^- \rightarrow W^-e^-\nu_e, \quad (4)$$

$$e^-e^- \rightarrow Z^0e^-e^-. \quad (5)$$

The cross sections for these processes have been computed and discussed previously [9, 10]. They are of the order of 1 pb.

Going still one power higher in the fine structure constant α , one encounters, among numerous other processes, pair production of weak gauge bosons:

$$e^-e^- \rightarrow W^+W^-e^-e^-, \quad (6)$$

$$e^-e^- \rightarrow W^-W^-\nu_e\nu_e, \quad (7)$$

$$e^-e^- \rightarrow W^-Z^0e^-\nu_e, \quad (8)$$

$$e^-e^- \rightarrow Z^0Z^0e^-e^-. \quad (9)$$

Although these reactions do not take place very frequently (at least at lower energies), they may be a source of dangerous background to rare exotic processes such as the examples contemplated in section 2.

In the following we will focus on the weak boson pair production processes (7) to (9) [2, 3]. Especially reaction (7) is very important, since it mimics the final state of $e^-e^- \rightarrow W^-W^-$.

But also reactions (8) and (9), depending on the W^- and Z^0 decay channels, may give rise to irreducible background.

The different topologies of Feynman diagrams contributing to weak boson pair production are exemplified in Fig. 4. In addition to double Bremsstrahlung diagrams represented in Fig. 4a, there are diagrams involving the triple gauge boson couplings as in Figs 4b, c, d and f, gauge-Higgs boson couplings as in Figs 4e and g, and the quartic gauge boson couplings as in Fig. 4h. The actual diagrams can be easily constructed from these generic ones by an appropriate particle assignment and by permutations of the momenta of identical particles. In the limit of zero electron mass, one has 66, 88 and 86 diagrams in the $W^-W^-\nu_e\nu_e$, $W^-Z^0e^-\nu_e$ and $Z^0Z^0e^-e^-$ channels, respectively. In reaction (7), each of the two fermion lines is coupled to a W^- boson, so that only the LL combination of initial polarizations has a non-zero cross section. For reaction (8), also the LR combination of beam polarizations is relevant, whereas the unpolarized cross section of reaction (9) receives contributions from LL , LR and RR beam polarizations.

When the traditional trace technique is employed, not only does the number of terms become prohibitive, but one also observes large gauge cancellations between them. For these reasons, we directly calculate helicity amplitudes using two different methods and square them numerically. In diagrams in which a virtual photon is coupled to an on-shell electron line, the neglect of the electron mass leads to collinear singularities. In these cases, regulating terms proportional to m_e^2 are kept in the photon propagator. Moreover, in order to obtain better numerical convergence of the Monte Carlo integration, we introduce new variables which smooth out the singular behaviour of the amplitudes in the collinear regions. For further details of the calculation of the matrix elements and the phase space integrations we refer to [2, 3].

In Fig. 5 we show numerical predictions⁴ for the total unpolarized cross sections of reactions (7) to (9) as a function of the e^-e^- centre-of-mass energy. The following values are used for the electroweak parameters: $m_Z = 91.19$ GeV, $m_W = 80.3$ GeV, $\sin^2\theta_W = 0.2244$, and $\alpha(m_Z^2) = 1/128.87$. Concerning $\alpha(Q^2)$, there is some uncertainty related with the ambiguity of the choice of the scale Q^2 , a typical problem in t -channel processes. For the Higgs boson mass we take $m_H = 100$ GeV. However, this choice has practically no influence on the numerical results (except in reaction (9), where a Higgs boson heavier than two Z^0 masses can be produced resonantly; we do not contemplate this possibility here). It is interesting to note the occurrence of subtle gauge cancellations involving triple and quartic gauge boson couplings, which reduce individual contributions from gauge invariant subsets of Feynman diagrams by up to 3 orders of magnitude.

Assuming a realistic integrated luminosity of 10 fb^{-1} per year, we expect about 25 $W^-W^-\nu_e\nu_e$, 100 $W^-Z^0e^-\nu_e$, and 10 $Z^0Z^0e^-e^-$ events at $\sqrt{s} = 500$ GeV. With increasing energy the yield of weak boson pairs becomes much larger. This holds especially for reactions (7) and (8) the cross sections of which rise to several tens to hundreds of fb above 1

⁴After this talk was presented, we learned of two other recent calculations [15] of these processes, which confirm the results presented here.

TeV. Hence, comparing these rates with the cross sections for exotic processes in Eq. (2) and Fig. 3, one has to worry about the question whether or not standard gauge boson pair production can obscure interesting new physics.

Fortunately, a study of the differential distributions for reactions (7–9) shows that this background can be eliminated by imposing relatively simple kinematical cuts. We illustrate this assertion for the process $e_L^- e_R^- \rightarrow W^- Z^0 e^- \nu_e$ in Fig. 6 by displaying the distributions of the transverse momentum and energy of the $W^- Z^0$ pair at $\sqrt{s} = 0.5$ and 2 TeV. We see that at $\sqrt{s} = 0.5$ TeV the energy distribution of the $W^- Z^0$ pair assumes its maximum slightly above $0.5\sqrt{s}$ whereas the transverse momentum distribution of the gauge boson pair peaks at about $0.1\sqrt{s}$. At $\sqrt{s} = 2$ TeV, both distributions are slightly softer. The peaking of the transverse momentum distribution becomes more pronounced at $\sqrt{s} = 2$ TeV showing that the gauge bosons tend to be emitted more and more along the beam axis as the energy increases. Another important observation which can be exploited for discrimination is the fact that, at both centre-of-mass energies, the $W^- Z^0$ energy distribution dies out almost completely for $E_{W^-} + E_{Z^0} > 0.8\sqrt{s}$. Thus, a simple cut imposed on the sum of gauge boson energies should help to eliminate these processes as a background to most of exotic reactions, in particular to $e^- e^- \rightarrow W^- W^-$, where the gauge bosons would carry almost the whole centre-of-mass energy.

These features are independent of initial state polarization and hold for all processes (7) to (9). Polarized cross sections and differential distributions in other interesting variables are given in [2, 3].

4 Conclusions

The $e^- e^-$ option of a linear collider provides novel possibilities to search for new physics. Especially lepton-number violating processes can be probed with high sensitivity. The standard model backgrounds mainly arise from single and pair production of weak gauge bosons. The cross sections and differential distributions of these processes can be evaluated with good accuracy. Hence, the expected numbers of events can be estimated reliably. In addition, these backgrounds can be substantially reduced by imposing relatively simple cuts on angles and energies.

In the TeV energy range, the cross sections for $e^- e^- \rightarrow W^- e^- \nu_e$, $e^- e^- \rightarrow Z^0 e^- e^-$, $e^- e^- \rightarrow W^- W^- \nu_e \nu_e$ and $e^- e^- \rightarrow W^- Z^0 e^- \nu_e$ become large enough to allow for interesting studies of the gauge nature of the standard model if luminosities of 10 fb^{-1} are reached. Such tests are particularly interesting in $W^- W^-$ and $W^- Z^0$ pair production where triple and quartic gauge boson couplings contribute at the same time.

References

- [1] Proceedings of the Workshop – Munich, Annecy, Hamburg, 1992 – 1993, e^+e^- *Collisions at 500 GeV: The Physics Potential*, DESY 92-123A, 92-123B, 93-123C.
- [2] F. Cuypers, K. Kołodziej, O. Korakianitis, R. Rückl, Phys. Lett. B325 (1994) 243.
- [3] F. Cuypers, K. Kołodziej, R. Rückl, preprint MPI-PhT/94-27, LMU-06/94.
- [4] D. London, G. Belanger, J.N. Ng, Phys. Lett. B188 (1987) 155.
- [5] C.A. Heusch, P. Minkowski, Nucl. Phys. B416 (1994) 3.
- [6] J. Maalampi, A. Pietilä, J. Vuori, Phys. Lett. B297 (1992) 327.
- [7] P.H. Frampton, D. Ng, Phys. Rev. D45 (1992) 4240.
- [8] J. Maalampi, A. Pietilä, M. Raidal, Phys. Rev. D48 (1993) 4467.
- [9] F. Cuypers, G.J. van Oldenborgh, R. Rückl, Nucl. Phys. B409 (1993) 128.
- [10] D. Choudhury, F. Cuypers, Phys. Lett. B325 (1994) 500;
D. Choudhury, F. Cuypers, Munich preprint MPI-Ph/94-24 (Nucl. Phys. B, in press).
- [11] W.-Y. Keung, L. Littenberg, Phys. Rev. D28 (1983) 1067.
- [12] D. Choudhury, F. Cuypers, A. Leike, Munich preprint MPI-Ph/94-23.
- [13] F. Cuypers, Yad. Fis. **56** (1993) 23.
- [14] H.E. Haber, G.L. Kane, Phys. Rep. 117 (1985) 75;
H.P. Nilles, Phys. Rep. 110 (1984) 1.
- [15] V. Barger, J.F. Beacom, K. Cheung, T. Han, Madison preprint MAD-PH-779;
E. Boos, M. Dubinin, private communication.

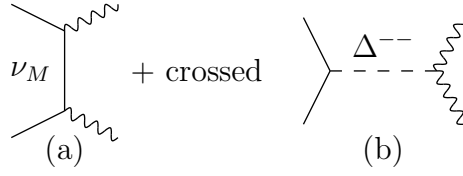


Figure 1: Feynman diagrams for $e^-e^- \rightarrow W^-W^-$; ν_M and Δ^{--} denote a heavy neutrino mass eigenstate and a doubly charged Higgs boson, respectively.

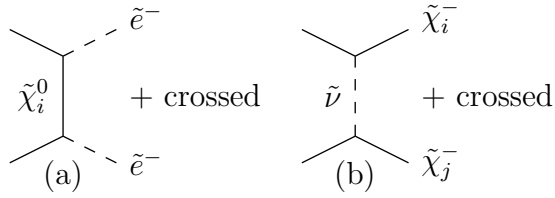


Figure 2: Feynman diagrams for the supersymmetric reactions $e^-e^- \rightarrow \tilde{e}^-\tilde{e}^-$ (a) and $e^-e^- \rightarrow \tilde{\chi}_i^-\tilde{\chi}_j^-$ (b).

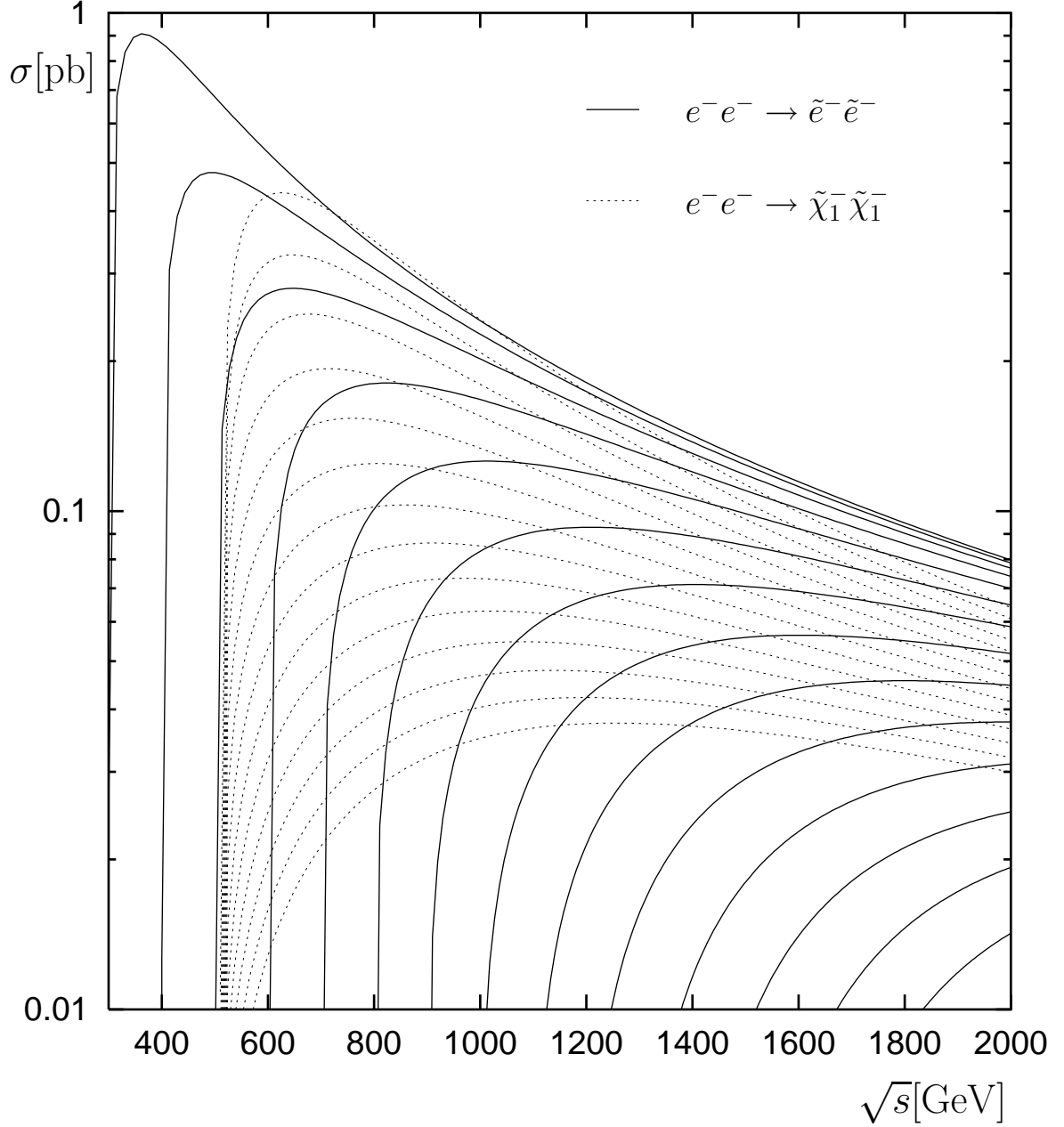


Figure 3: Energy dependence of the unpolarized production cross sections of $e^-e^- \rightarrow \tilde{e}^-\tilde{e}^-$ (full curves) and $e^-e^- \rightarrow \tilde{\chi}_1^-\tilde{\chi}_1^-$ (dotted curves) for $m_{\tilde{e}} = m_{\tilde{\nu}} = 150, 200, \dots, 800$ GeV, assuming $\tan\beta = 10$, $\mu = -300$ GeV and $M_2 = 300$ GeV. For this choice of parameters, $m_{\tilde{\chi}_1^-} = 255$ GeV.

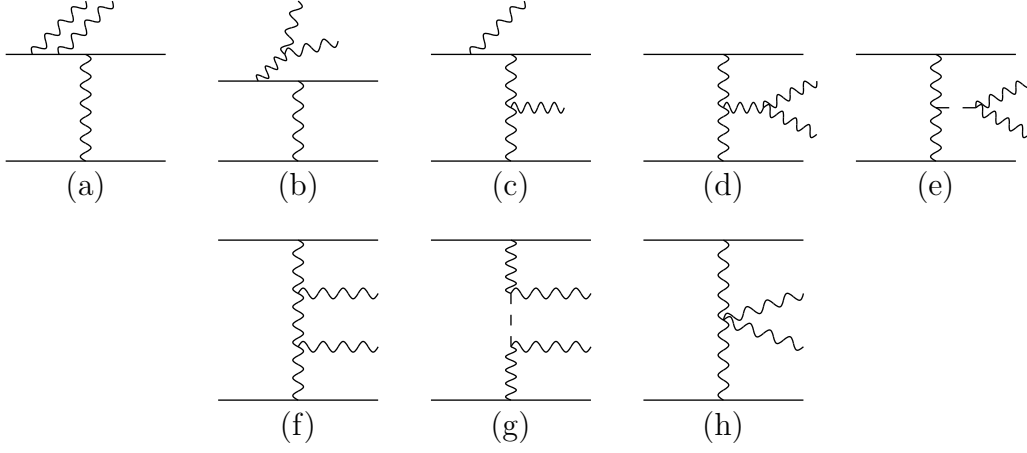


Figure 4: Typical topologies of the Feynman diagrams of weak boson pair production reactions.

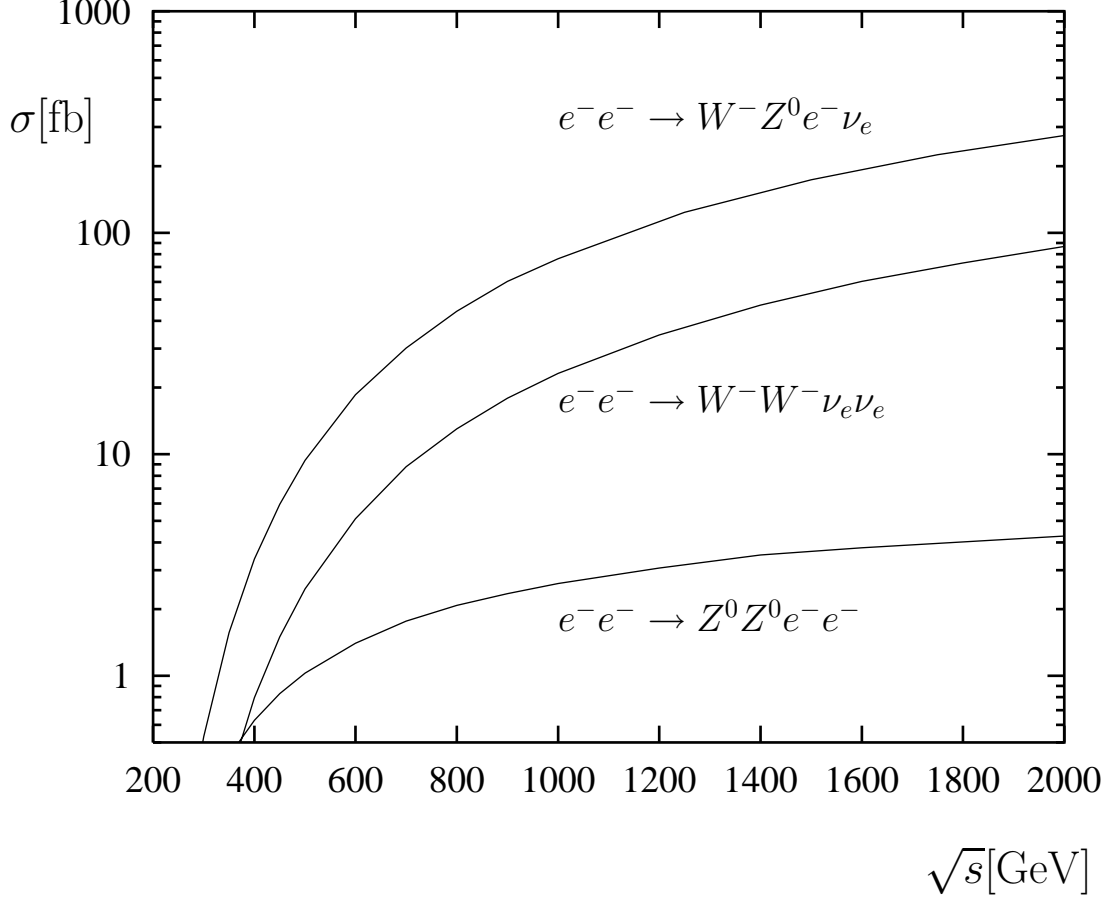


Figure 5: Total cross sections for gauge boson pair production with unpolarized e^- beams.

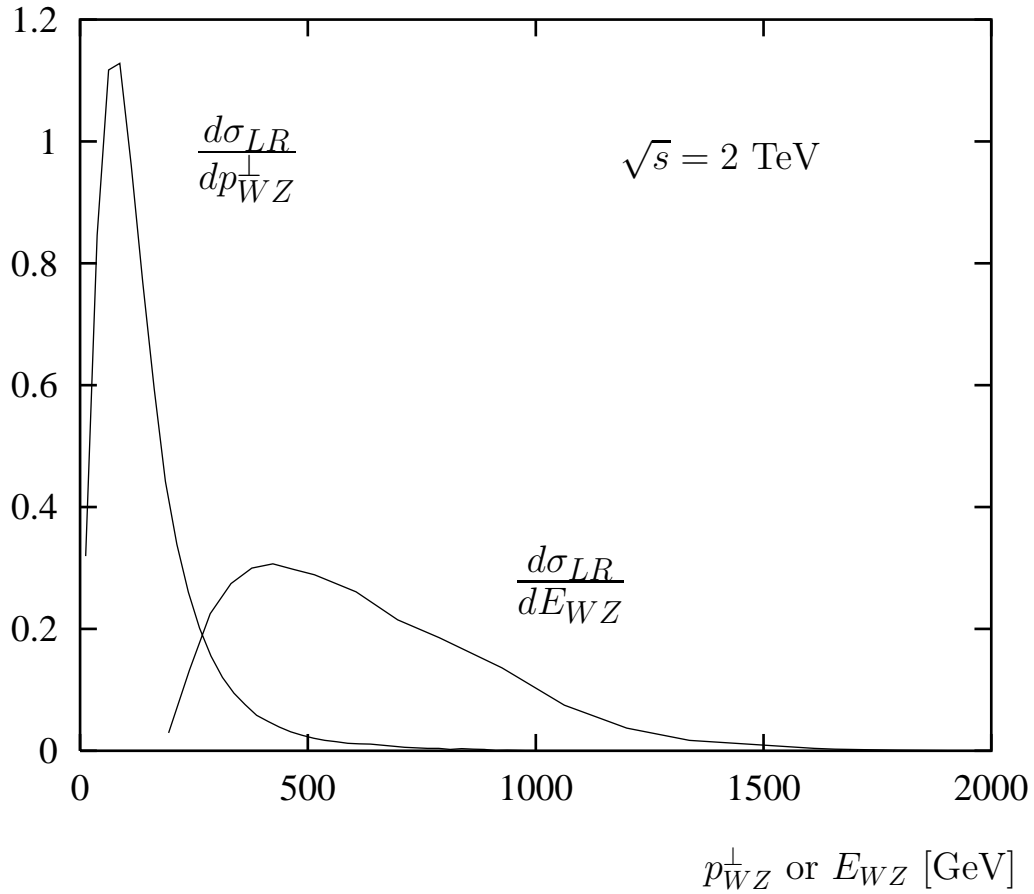
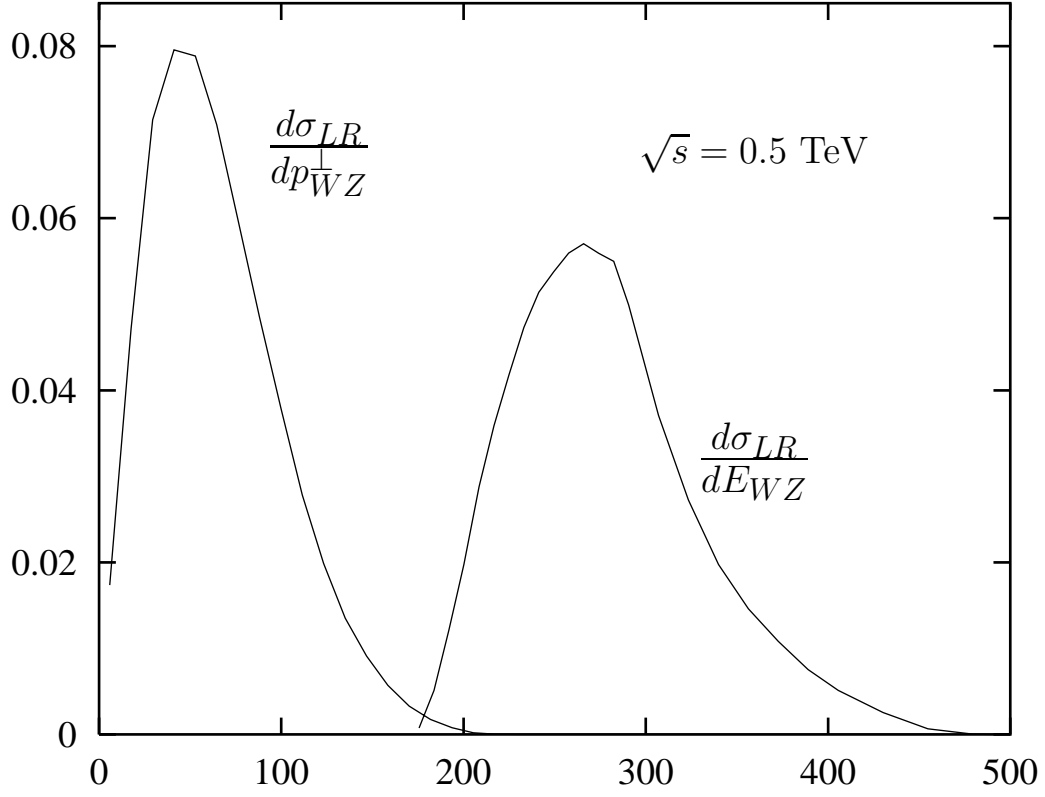


Figure 6: Transverse momentum and energy distributions of the $W^- Z^0$ -pair in $e_L^- e_R^- \rightarrow W^- Z^0 e^- \nu_e$ in fb/GeV.